



Effect of Na₂O on aqueous dissolution of nuclear waste glasses



Rahmat Ullah Farooqi^{a, *}, Pavel Hрма^{a, b}

^a Division of Advanced Nuclear Engineering, Pohang University of Science and Technology, 77 Cheongam-Ro, Nam-Gu, Pohang, Gyeongbuk 790-784, Republic of Korea

^b Pacific Northwest National Laboratory, Richland, WA, United States

ARTICLE INFO

Article history:

Received 24 October 2016

Received in revised form

6 February 2017

Accepted 6 February 2017

Available online 7 February 2017

Keywords:

Glass durability

Mathematical model

Product consistency test

Acceptability limits

B and Na releases

Component effects

Composition region

ABSTRACT

Sodium oxide is present in the majority of commercial and waste glasses as a viscosity-reducing component. In some nuclear waste glasses, its source is the waste itself. As such, it can limit the waste loading because of its deleterious effect on the resistance of the glass to attack by aqueous media. The maximum tolerable content of Na₂O in glass depends on the presence and concentration of components that interact with it. To assess the acceptability limits of Na₂O in the composition region of nuclear waste glasses, we formulated 11 baseline compositions by varying the content of oxides of Si, B, Al, Ca, Zr, and Li. In each of these compositions, we varied the Na₂O fraction from 8–16 mass% to 23–30 mass%. To each of 146 glasses thus formulated, we applied the seven-day Product Consistency Test (PCT) to determine normalized B and Na releases (r_i , where $i \equiv B$ or Na). Fitting approximation functions $\ln(r_i/gm^{-2}) = \sum b_{ij}g_j$ to r_i data (g_j is the j -th component mass fraction and b_{ij} the corresponding component coefficient), we showed that the r_B (and, consequently, the initial glass alteration rate) was proportional to the glass component mass fractions in the order Al₂O₃<CaO<SiO₂<ZrO₂<B₂O₃<Na₂O<Li₂O. No threshold was detected at which glass structure would fall apart or beyond which a continuous nondurable phase would be separated. Specific examples are given to demonstrate restrictions imposed on the boundary of the composition region of acceptable glasses by the maximum allowable r_B and by the melt viscosity required for glass melter operation. Finally, the role that PCT data may play in understanding the evolution of the glass alteration process is discussed.

© 2017 Elsevier B.V. All rights reserved.

1. Introduction

The attack of aqueous media on glass is a complex process in which water functions as a catalyst that allows the thermodynamically unstable, yet kinetically frozen, amorphous material to be converted to various more stable minerals, such as clays and zeolites. Glass corrosion never stops as long as the glass is exposed to a humid environment. Substantial progress in understanding its mechanism and kinetics has been achieved in recent decades in connection with assessment of the long-term performance of nuclear waste glasses [1–3]. The glass alteration is influenced by glass structure, the aqueous medium, and most notably by interfacial layers that form on the glass-water interface, which consist of multiple sublayers, from altered glass through stratified gels to precipitated minerals [2,4]. The innermost densified layer can

become protective [1]. Glass affects its interaction with water both at the atomic and the nanoscale level, at which ions form chemical groupings of various atomic arrangements [5] that may, in extreme cases, be organized into channels or two-dimensional regions of concentrated network modifiers [6]. The aqueous medium can contain pH buffers, organic substances, ions from glass corrosion products, and environmental minerals, which may originate from the groundwater or be deliberately added.

Depending on the physical and chemical circumstances, which may change over time, the alteration process undergoes several stages from the initial rapid change to the rate-drop period and the final stage of the nearly constant residual rate [7], though one or several temporary accelerations may occur [3,8].

Understanding the interaction of glass with aqueous media is a challenging endeavor even with a glass of a unique well-defined composition, such the R7T7 glass designed for commercial radioactive waste [9]. For Hanford glasses to be formulated for the vitrification of nuclear wastes from plutonium production [10], the number of compositions runs to several thousand. Here we deal not

* Corresponding author.

E-mail address: rufarooqi@live.com (R.U. Farooqi).

just with individual compositions but with a composition region, a manifold embedded in multidimensional composition space. Though the effects of minor chemical constituents can be neglected, the number of influential components is high, typically 10 to 20. Glass properties, such as viscosity, are then expressed, using approximation relationships, as functions of glass composition and possibly other relevant variables such as temperature.

To understand the roles of individual chemical constituents—mostly oxides, but also halogens (F, Cl) and elements (Pd)—in glass alteration process, gross simplifications in both materials and physico-chemical test conditions are needed before important secondary phenomena are identified and dealt with. Glasses of as few as three components have been studied in depth, mainly to clarify the effects of glass structure on the early stages of corrosion. Glasses with just a few basic components were recently promoted as International Simplified Glasses intended predominantly for the study of the influence of the basic oxides on long-term corrosion through experiments lasting for several decades [11]. Simplified test conditions consist of drastic reductions of test variables, i.e., temperature, glass surface-to-solution volume ratio, solution pH, solution composition, and test duration, either under static or dynamic (flow-through) conditions; these variables are kept constant or allowed to change in response to the reaction progress.

Whereas the long-term rate of alteration is the ultimate criterion of waste glass quality, the practical aspects of glass acceptability for disposal make it necessary to design specific short-term tests that glasses considered for disposal must pass. One such test is the product consistency test (PCT) [12] used as a criterion for acceptance of U.S. waste glasses for disposal, and is the focus of this research as an example for investigating broader corrosion rate-composition relationships.

In this study, we focus on the effect of the Na₂O fraction on the glass alteration short-term response. Na₂O is present in the majority of commercial glasses as a viscosity-reducing component. In some nuclear waste glasses, Na₂O comes from the waste itself and can limit the waste loading because of its deleterious effect on resistance of the glass to attack by aqueous media. This way, Na₂O limits the composition region of acceptable waste glasses.

The maximum tolerable content of Na₂O in glass depends on the degree to which the glass structure is weakened by nonbridging oxygen or by nanoscale phase separation. The effect of Na₂O on glass structure depends on the content of other oxides that interact with it. As described in Section 2.1, we designed 11 baseline glasses, varying oxides of Si, B, Al, Ca, and Zr, of which we designed two series, one without Li₂O and the other with 5 mass% Li₂O. By changing the Na₂O fraction from 10 to 28 mass% (occasionally from 8 to 30 mass%), typically in steps of 2 mass%, we formulated and tested 146 compositions.

A study with a large number of compositions requires simple well-defined test conditions and a precisely specified and meticulously executed test method. In selecting such a method for assessing glass alteration response, we considered two types of requirements. The first was to design experiments that would allow us to determine whether the transition from highly durable to exceedingly less durable glasses (associated with an increasing content of Na₂O) is smooth and continuous or whether it rapidly increases after exceeding a threshold that can be associated with the glass structure becoming more heterogeneous. Ledieu et al. [13] observed a rapid increase of dissolved fractions of Na₂O and B₂O₃ when the content of Na₂O + B₂O₃ exceeded ~30 mol% in sodium borosilicate glass, and attributed this abrupt change to the formation of a nanoscale sodium-borate interconnected network from which the soluble components were extracted. Does nanoscale phase segregation exist in sodium borosilicate glasses containing

more than three components? If so, this would impose limits on the composition region of acceptable glasses. Unlike alteration resumption, which occurs only after the solution becomes oversaturated with respect to analcime formation [8], nanoscale sodium borate phase would accelerate the initial rate of corrosion, and thus would be detected with the PCT.

The second requirement was associated with our resolve to make the outcome comparable with existing data that have been accumulated during the development of nuclear waste vitrification technology dealing with expansive composition regions, as is the case with the Hanford Tank Waste Treatment and Immobilization Plant (WTP). Two types of glasses will be produced at Hanford: high-level waste (HLW) glasses containing water-insoluble waste components plus Cs, and low-activity waste (LAW) glasses from the tank supernatant containing predominantly sodium nitrates, hydroxides, and nitrites [10].

Because Li₂O is a common component of Hanford HLW glasses and is present in some LAW glasses, we added Li₂O to about 60% of the test compositions. For the LAW, it is desirable to formulate durable glasses with the maximum possible content of Na₂O. This need motivated our experimental design of testing glasses with high Na₂O fractions and zero Li₂O content—apart from the primary motivation to look for a possible discontinuity in the glass alteration response to composition.

Regarding the test method (Section 2.2), we chose the PCT. This test is widely used for the acceptability of nuclear waste glasses in the United States. An extensive database of PCT results is available encompassing a large composition region [10]. The test is fastidiously defined by ASTM [12], eliminating every possible uncontrolled variable that could affect the data. Therefore, when the glass composition is the only controlled variable, the results would solely reflect its effects, and thus mathematical models relating the test outcome to glass composition can be constructed (Sections 2.3 and 3). The drawback of such an approach is that the corrosion mechanism and kinetics are not addressed when a single test is used. These limitations are discussed in Section 4.2.

2. Experimental

2.1. Composition region

Ideally, the experimental composition region should be large enough to include glasses that are likely to be produced. In this study, we focused on the effect of Na₂O on the PCT response. To this end, we somewhat narrowed the composition ranges of other major glass components, but kept them wide enough for reliably fitting empirical models to data (Section 3). At the same time, we extended the range of Na₂O fractions far beyond the acceptability limits so we could identify the boundaries of the composition region on which the glass has acceptable properties (Section 4.1).

The test glass compositions were simplified by maintaining only seven essential components: SiO₂, B₂O₃, CaO, Al₂O₃, ZrO₂, Na₂O, and Li₂O. By varying five of these components, SiO₂, B₂O₃, CaO, Al₂O₃, and ZrO₂, one at a time, we formulated two sets of 11 baseline glasses (Table 1), one set with 23 mass% Na₂O and zero Li₂O and the other with 18 mass% Na₂O and 5 mass% Li₂O. In each baseline glass, we then varied the Na₂O fraction starting from 8–16 mass% and advancing to 23–30 mass% in steps of mostly 2 mass% while keeping the remaining components in constant proportions, thus formulating the total number of 146 compositions (91 with ~5 mass% Li₂O and 55 without Li₂O), see Tables A1 and A2 in the Appendix. The composition region of the test glasses is shown in Table 2.

Table 1

Composition of baseline glasses in mass fractions; the sum of Na₂O and Li₂O mass fractions was 0.23 in each glass. Components are varied one at a time as indicated by bold italicized numbers.

ID	SiO ₂	B ₂ O ₃	Al ₂ O ₃	ZrO ₂	CaO
CT-S50-N18	0.5000	0.1200	0.0500	0.0600	0.0400
CT-S40-N18	0.4000	0.1644	0.0685	0.0822	0.0548
CT-S30-N18	0.3500	0.1867	0.0778	0.0933	0.0622
CT-B16-N18	0.4692	0.1600	0.0469	0.0563	0.0375
CT-B08-N18	0.5308	0.0800	0.0531	0.0637	0.0425
CT-A08-N18	0.4792	0.1150	0.0800	0.0575	0.0383
CT-A11-N18	0.4583	0.1100	0.1100	0.0550	0.0367
CT-Z03-N18	0.5211	0.1251	0.0521	0.0300	0.0417
CT-Z09-N18	0.4789	0.1149	0.0479	0.0900	0.0383
CT-C00-N18	0.5274	0.1266	0.0527	0.0633	0.0000
CT-C08-N18	0.4726	0.1134	0.0473	0.0567	0.0800

Table 2

Experimental composition region of the test glasses in mass fractions.

	Maximum	Minimum	Average
SiO ₂	0.5917	0.3073	0.4715
B ₂ O ₃	0.2061	0.0702	0.1291
Al ₂ O ₃	0.1214	0.0412	0.0611
ZrO ₂	0.1030	0.0263	0.0646
CaO	0.0883	0.0000	0.0417
Na ₂ O	0.3000	0.0800	0.2020
Li ₂ O	0.0561	0.0000	0.0301

2.2. Glass preparation, glass testing, and data evaluation

Glasses were batched using analytical-grade chemicals SiO₂, H₃BO₃, Al(OH)₃, Zr(OH)₄, CaCO₃, Na₂CO₃, and Li₂CO₃. Batches were melted in platinum crucibles for 1–2 h at either 1000–1100 °C (glasses with Li₂O) or 1150–1550 °C (lithium-free glasses). The seven-day PCT was performed following the ASTM procedure. The glasses were ground and sieved to produce powder of 75–150 μm grain size. The powder was ultrasonically cleaned, three times with water and then twice with ethanol, and finally dried in oven at 105 °C. The amount of 1.5 g glass was mixed with 15 ml deionized water in a teflon vessel and kept in an oven at 90(±2)°C for 7 days. The solution was filtered (Whatman syringe filters, 0.45 μm pore size) and analyzed with inductively coupled plasma atomic emission spectroscopy. Normalized releases of elements were computed using the formula $r_i = (c_i - c_{Bi})/(g_i\sigma)$, where r_i is the i -th element normalized release, c_i is the i -th element concentration in the solution, c_{Bi} is the i -th element concentration in the blank, g_i is the i -th element mass fraction in the glass, and σ is the initial glass surface area-to-solution volume ratio ($\sigma \sim 2000 \text{ m}^{-1}$). Note that both glass surface area and solution volume change as a result of glass alteration, but the system is isolated in a tightly closed vessel.

2.3. Model design

The following approximation function was fitted to data by linear regression:

$$\ln(r_i) = \sum_{j=1}^N b_{ij}g_j \quad (1)$$

where r_i is the i -th element normalized release ($i \equiv \text{B or Na}$), g_j is the j -th component mass fraction in glass, b_{ij} is the i -th element coefficient for the j -th component, and N is the number of components. This type of approximation function is common for PCT data except that a few higher-order terms are added on the right-hand side of

Equation (1) for many-component glasses [10]. Frugier et al. [14] used r_i values (instead of their logarithm) for the initial alteration rate as a function of composition. The relationship between r_i and glass composition was highly nonlinear and a second-order polynomial had to be used to obtain a reasonable fit.

3. Results

Fig. 1 displays r_B data versus the temperature at which the molten glass viscosity would be 5 Pa s as estimated with a recently published glass model [15]. The Li-containing glasses (blue circles) melted at lower temperatures and had higher r_B values (lower corrosion resistance) than glasses with zero Li content (red diamonds). Note that the outliers occur around extreme r_B values of each group (~5 mass% Li₂O and 0 mass% Li₂O). The horizontal lines indicate r_B values of 2 and 50 g m⁻², the relevance of which is explained below. The vertical lines drawn at $T = 1050$ °C and 1200 °C indicate processability constraints of Joule-heated melter (roughly equivalent to $\eta = 2$ and 8 Pa s at 1150 °C) discussed in Section 4.1.

Fig. 2 illustrates another remarkable feature of the data, namely that starting at $r_B \sim 7.5 \text{ g m}^{-2}$, the normalized sodium release rapidly decreased with growing r_B , i.e., the $r_{Na} - r_B$ difference becomes exceedingly negative. This effect has been reported previously [16]. The high releases—those with r_B higher than $\sim 7.5 \text{ g m}^{-2}$ —are most likely associated with the Na₂O retention in the gel layer; a selective leaching of alkali borates from nano-segregated glasses can be ruled out as their cause.

Several sets of b_{Bj} and $b_{Na,j}$ coefficients were obtained by fitting Eq. (1) to the measured r_B and r_{Na} data. The sets, shown in Tables 3 and 4, differ only in data selected for fitting: Eq. (1) was fitted to all data (models B1 and Na1), all data minus outliers (models B2 and Na2), data for glasses with Na₂O mass fraction ≤ 0.24 (models B3 and Na3), and data for glasses with zero Li₂O content (models B4 and Na4). Models B3 and Na3 were included because it is currently considered that glasses with Na₂O mass fractions > 0.24 would not be designed for Hanford LAW glasses.

Note that the $b_{B,CaO}$ (Table 3) is significantly higher for zero-lithium glasses, indicating a possible CaO–Li₂O interaction. Another remarkable difference exists between $b_{Na,j}$ and $b_{B,j}$ coefficients for $j \equiv \text{CaO, Al}_2\text{O}_3, \text{ or B}_2\text{O}_3$. While $b_{Na,j}$ is significantly

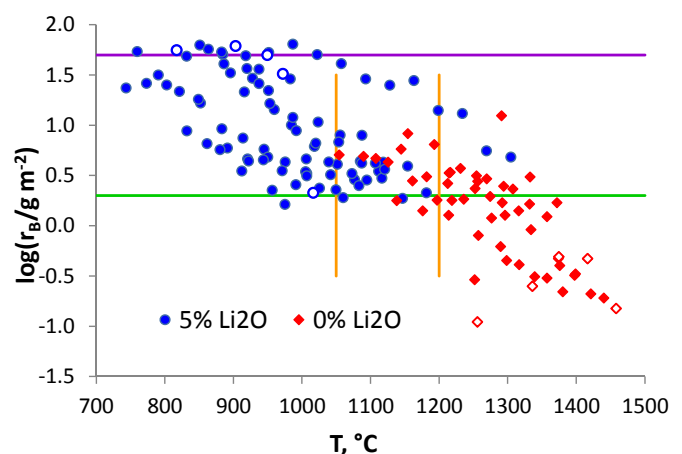


Fig. 1. Normalized B release versus estimated temperature at which melt viscosity is 5 Pa s; hollow data points indicate model B2 outliers (see Table 3); the horizontal lines indicate r_B values of 2 and 50 g m⁻²; the vertical lines drawn at $T = 1050$ °C and 1200 °C indicate processability constraints of Joule-heated melter (roughly equivalent to $\eta = 2$ and 8 Pa s at 1150 °C); note that decadic logarithms are used in graphs and natural logarithms in models, see Eq. (1).

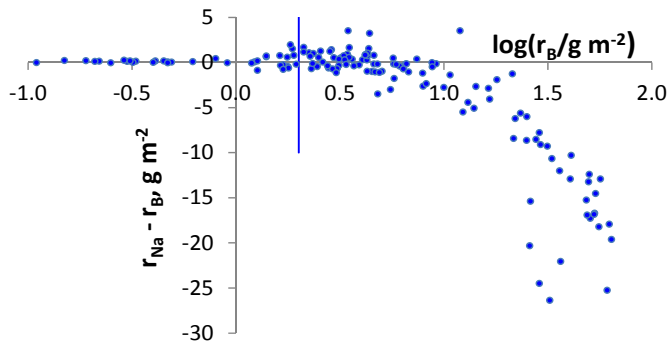


Fig. 2. Difference between sodium and boron normalized releases versus $\log r_B$; the vertical line at $r_B = 2 \text{ g m}^{-2}$ corresponds to a maximum value for which LAW glasses are customarily designed.

Table 3

The component coefficients for the normalized boron release (with standard errors in parentheses) and elementary statistics (R^2 and R^2_{adj} are correlation coefficients, ϵ is the standard error, n_t is the total number of data, n_s is the number of data selected for fitting, and n_o is the number of outliers).

Model	All data		<24 mass% Na ₂ O	0% Li ₂ O
	B1 ^a	B2 ^b	B3	B4
SiO ₂	−3.60 (0.44)	−3.02 (0.31)	−2.92 (0.34)	−4.72 (0.45)
B ₂ O ₃	14.21 (0.97)	16.37 (1.41)	16.25 (1.39)	16.87 (1.61)
Al ₂ O ₃	−27.69 (2.87)	−28.76 (2.03)	−26.37 (2.03)	−26.32 (2.19)
ZrO ₂	−4.09 (3.23)	−0.93 (2.37)	3.43 (2.41)	−6.18 (2.71)
CaO	−18.77 (2.71)	−25.11 (2.05)	−25.87 (2.02)	−9.64 (3.18)
Na ₂ O	15.94 (1.19)	14.72 (0.85)	12.52 (1.11)	15.89 (1.64)
Li ₂ O	29.94 (2.22)	25.50 (1.62)	23.46 (1.59)	
R^2	0.842	0.910	0.892	0.914
R^2_{adj}	0.836	0.906	0.886	0.903
ϵ	0.610	0.426	0.395	0.313
n_s	146	136	114	48
n_t	146	146	122	55
n_o	0	10	8	7

^a Eq. (1) was fitted to all data including outliers.

^b Eq. (1) was fitted to all data minus outliers.

Table 4

The component coefficients for the normalized sodium release and elementary statistics. See Table 3 for the symbol definitions.

Model	All data		<24 mass% Na ₂ O	0% Li ₂ O
	Na1 ^a	Na2 ^b	Na3	Na4
SiO ₂	−3.08 (0.39)	−2.70 (0.30)	−2.87 (0.32)	−5.05 (0.42)
B ₂ O ₃	9.39 (1.73)	9.79 (1.33)	9.65 (1.32)	9.16 (1.61)
Al ₂ O ₃	−19.69 (2.51)	−21.30 (1.93)	−19.36 (1.93)	−19.03 (2.17)
ZrO ₂	−4.87 (2.83)	−0.16 (2.23)	2.48 (2.24)	−6.81 (2.80)
CaO	−12.31 (2.37)	−16.46 (1.94)	−17.29 (1.93)	−1.56 (2.47)
Na ₂ O	13.82 (1.04)	13.51 (0.80)	12.67 (1.04)	17.58 (1.57)
Li ₂ O	29.79 (1.95)	25.64 (1.56)	25.25 (1.5)	
R^2	0.843	0.892	0.876	0.884
R^2_{adj}	0.837	0.888	0.869	0.870
ϵ	0.535	0.408	0.376	0.312
n_s	146	140	115	50
n_t	146	146	122	55
n_o	0	6	7	5

^a Eq. (1) was fitted to all data including outliers.

^b Eq. (1) was fitted to all data minus outliers.

higher than $b_{B,j}$ for $j \equiv \text{CaO}$ or Al_2O_3 , the difference is opposite for $j \equiv \text{B}_2\text{O}_3$. Thus, the contents of these three oxides are a dominant influence on the $r_{\text{Na}} - r_B$ difference (Fig. 2). In glasses with the $r_{\text{Na}} - r_B$ close to zero, $(\text{CaO} + \text{Al}_2\text{O}_3)/\text{B}_2\text{O}_3 < 0.8$ (in terms of mass fractions) whereas $(\text{CaO} + \text{Al}_2\text{O}_3)/\text{B}_2\text{O}_3 > 1$ for most glasses with $r_{\text{Na}} - r_B < 0$.

Perhaps the most remarkable observation is that a simple first-order polynomial model, Eq. (1), represents data over the full experimental composition region (Table 2) including Na₂O

fractions ranging from 8 to 30 mass%, i.e., for the B release from 0.1 to 64 g m^{-2} and the Na release from 0.1 to 45 g m^{-2} . As the component coefficients and the correlation coefficients indicate (Tables 3 and 4), the same linear model fitted durable glasses ($r_B < 2 \text{ g m}^{-2}$) and nondurable glasses ($r_B > 2 \text{ g m}^{-2}$) equally well ($r_B = 2 \text{ g m}^{-2}$ is a maximum value for which LAW glasses are customarily designed—see a horizontal line in Fig. 1 and the vertical line in Fig. 2). Therefore, no nanoscale level separation by groupings of ions occurred to an extent that would cause an abrupt transition from congruent dissolution to leaching.

Fig. 3 displays estimated (subscript E) versus measured (subscript M) values and their cumulative squared differences versus number of data for model B2. Red diamonds indicate outliers. For boron releases, outliers occur at r_B values that are extremely low or extremely high; for sodium releases, outliers are

only located at the high durability (low r_{Na} values) end. As Fig. 4 demonstrates, outliers are not associated with the alkali content in glass. The absence of outliers at high values of Na release can be attributed to the high $r_B - r_{\text{Na}}$ differences seen in Fig. 2. The r_B values of the outlying durable glasses that are lower than the model predicted (those with low r_B values) are probably caused by volatilization from glasses that required high temperatures (up to 1500 °C) to melt (Fig. 1).

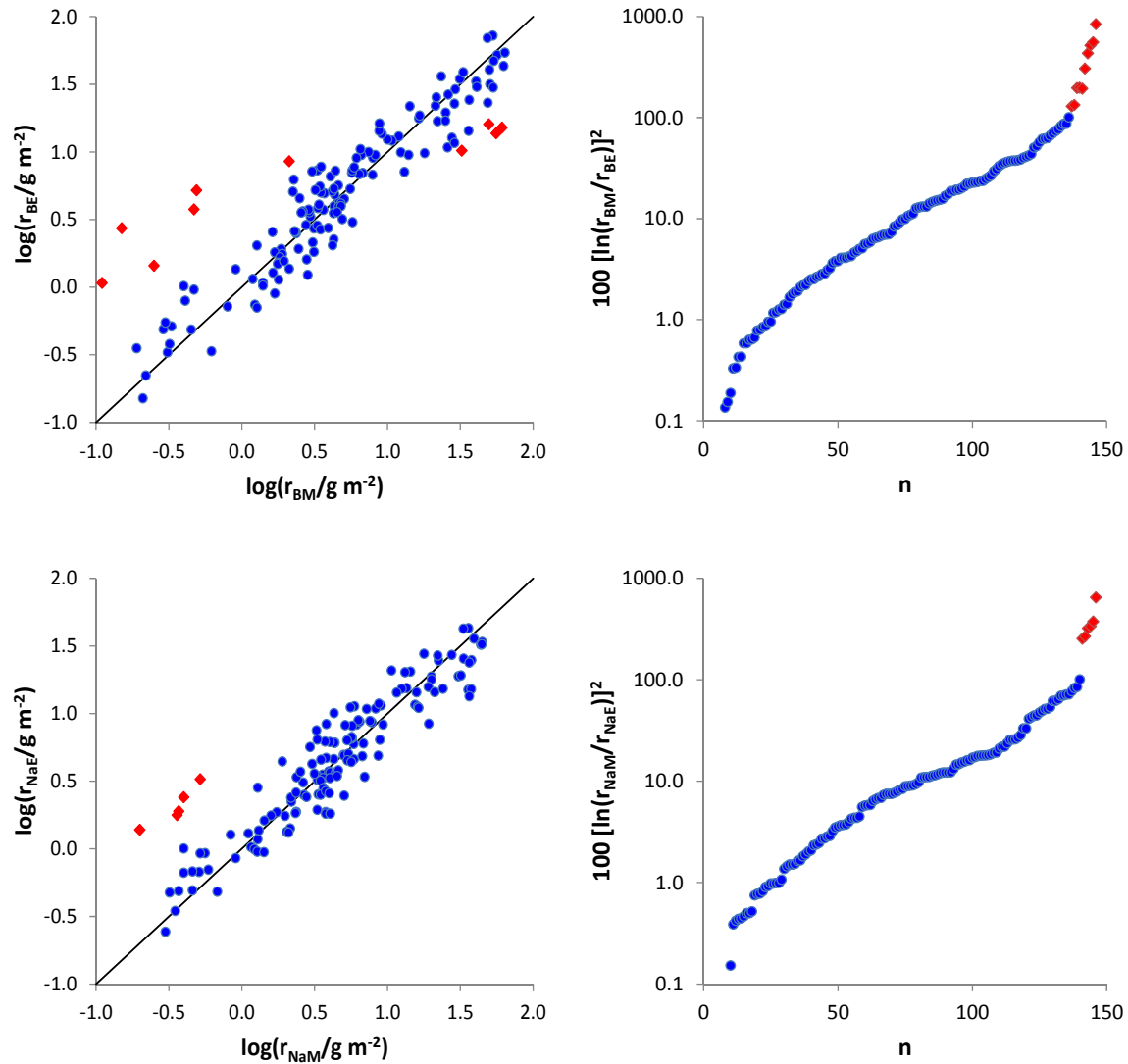


Fig. 3. Estimated (model B2) versus measured normalized B and Na releases (left plots) and the cumulative distribution of squared differences (right plots).

The maximum theoretical B release in the seven-day PCT is $m/(\sigma V)$ with $m = 1.5$ g, $V = 15$ ml, and $\sigma = 2000$ m^{-1} (Section 2.2), yielding 50 $g\ m^{-2}$ (marked by a horizontal line in Fig. 1). In this work, the maximum measured r_B and r_{Na} were 64 $g\ m^{-2}$ and 45 $g\ m^{-2}$, respectively. The r_B values exceeding the 50 $g\ m^{-2}$ limit indicate that the actual glass surface area was somewhat lower than $A = V\sigma = 3 \times 10^{-2}$ m^2 . The occurrence of high B release outliers (Fig. 3) indicates that some low-durability glasses altered somewhat faster than expected, turning all glass into alteration products at a time shorter than seven days, but it is unlikely that was caused by glass structural breakdown, phase separation, or corrosion acceleration associated with zeolite precipitation.

Fig. 5 shows component effects based on model B2. The lines indicate how the normalized B and Na releases change when individual oxides are added to or removed from the centroid composition with remaining components maintaining the same relative proportions. The average composition of all 146 glasses was selected as the centroid (B1 and B2 composition regions were identical and the averages differed by a few hundredths of a percent). Boron and sodium releases are most effectively decreased by Al_2O_3 , closely followed by CaO ; they are increased by Li_2O , followed by Na_2O and B_2O_3 . SiO_2 and ZrO_2 moderately

decrease the releases.

4. Discussion

Trouble-free processability and acceptable durability are criteria that nuclear waste glass must satisfy. For electric melters that operate at a fixed temperature, processability is defined by restrictions imposed on melt viscosity, segregation of molten and solid phases in the melter, and precipitation of solids during cooling [10]. The acceptability of glasses for long-term deposition is currently specified by means of short-term tests, of which the PCT has been established in the United States. Processability and acceptability determine the composition region the boundaries of which are defined by the limits imposed on glass properties (Section 4.1). Within this region, a glass is formulated that maximizes the waste loading (the fraction of waste components in glass).

Ideally, a durable glass should alter slowly enough that the release of radionuclides is not harmful to the environment. Though the long-term alteration of glass is subjected to current debate that has not yet reached a consensual conclusion and the physical and chemical circumstances to which the glass will be exposed over millennia cannot be determined with precision, substantial

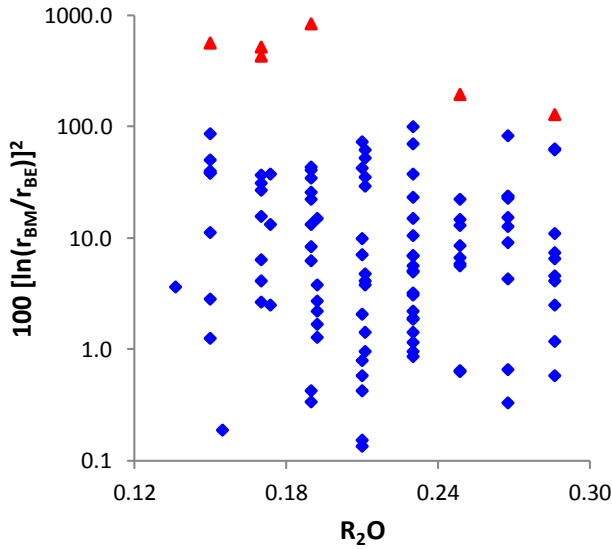


Fig. 4. Squared differences versus alkali content ($R_2O = Na_2O + Li_2O$); red triangles indicate outliers. (For interpretation of the references to colour in this figure legend, the reader is referred to the web version of this article.)

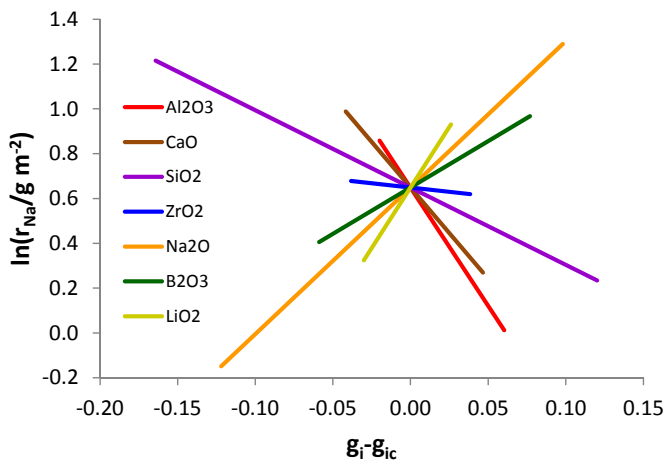
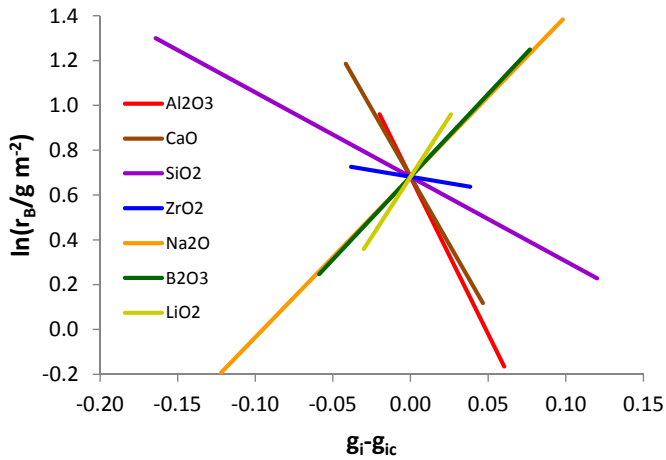


Fig. 5. Effects of glass components on r_B (top) and r_{Na} (bottom) when added to (or removed from) the centroid glass.

progress towards understanding the long-term alteration rate has been achieved. A larger database will be needed for the establishing the effects of glass composition on the full range of glass alteration progress (Section 4.2).

4.1. Composition region boundaries

One of the goals of this work was to determine the maximum fraction of Na_2O compatible with a restriction imposed on the r_B as an indicator of glass durability. Other constraints that restrict the number of degrees of freedom in selecting glass composition are melt viscosity, the tendency to crystallize, and the tendency to segregate molten salts, such as sulfate [10]. Although the number of waste glass components is high (40 or even higher), we control only the components added to any given waste, which total just a few. As the following two specific examples demonstrate, this relatively low number of degrees of freedom allows us to link the composition region boundaries with constraints imposed on glass and melt properties.

Example 1. Suppose that four additive components, SiO_2 , B_2O_3 , CaO , and Al_2O_3 , were selected for high-sodium waste vitrification. Let us assume that some other processability concerns (such as the sulfate content in the waste) restrict the Na_2O content to some maximum value and that the melt must have a specific viscosity value at a set temperature (this is a simplification; normally, we would deal with a viscosity range, usually 2–8 Pa s at 1150 °C; the vertical lines in Fig. 1 roughly correspond to these constraints). Thus, the four additive components plus Na_2O and the three constraining conditions (the mass balance, the constant viscosity, and the limited Na_2O content) leave us with two degrees of freedom, say the mass fractions of Al_2O_3 or CaO . Of course, the waste has more components than just Na_2O . Because waste components are at constant proportions, and thus the waste could be treated as a single component, we disregard other waste components for the sake of simplicity.

The graph of Fig. 6A depicts the composition region boundaries for glasses of a constant viscosity $\eta = 5$ Pa s at 1150 °C and $r_{B,max} = 2$ g m⁻². Solid lines represent glasses that contain 25 mass% Na_2O without increasing the r_B value above 2 g m⁻² for CaO mass fraction varying from 0 to 10 mass% (this range is wider than that of the experimental region, Table 2; such an extrapolation would be forbidden in an application, but is tolerable in an illustrative example). The graph was computed using a viscosity model given in Ref. [15] and component coefficients listed for model B4 in Table 3. As the red line shows, an increase in CaO content is compensated by a decrease in Al_2O_3 mass fraction. The green and blue lines show that B_2O_3 mass fraction decreases to keep the viscosity constant and SiO_2 mass fraction increases to maintain the mass balance requiring that the mass fractions of all components sum to 1.

Example 2. This is a variation on the previous example except that we assume that the glass contains ZrO_2 coming from the waste and that the PCT limit is more restrictive, constraining $r_{B,max}$ to 1 g m⁻². We have again just two degrees of freedom, as in the previous case, because the ZrO_2/Na_2O ratio is fixed by the waste composition. We use the same viscosity and r_B models as in Example 1.

Fig. 6B displays the result of the calculation. The solid lines represent $r_B = 1$ g m⁻², the dashed lines $r_B = 2$ g m⁻². The position of dashed lines with respect to solid lines demonstrates that a more restrictive condition on the PCT response requires a higher content of Al_2O_3 at a constant CaO content and vice versa. Because the Na_2O content is constant regardless of $r_{B,max}$, the change of the B_2O_3 fraction is small, responding to the change in $r_{B,max}$.

In these examples, we demarcated a composition region around

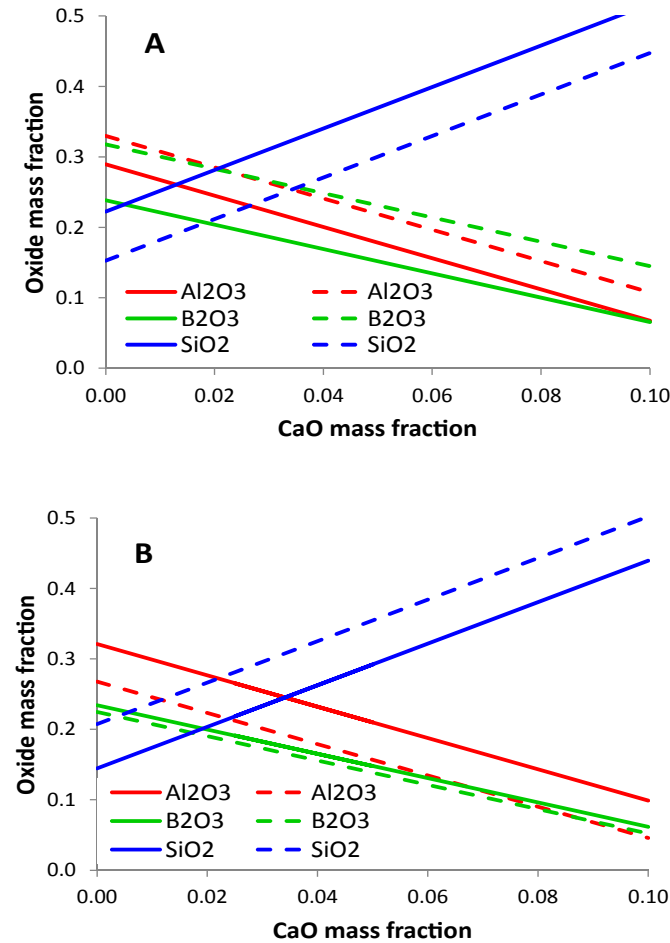


Fig. 6. Composition region boundary for glasses of viscosity 5 Pa s at 1150 °C. (A) The boundary is defined by the requirement that the PCT normalized B release $r_B \leq 2 \text{ g m}^{-2}$. Solid lines represent glasses containing 25 mass% Na_2O . Dashed lines represent glasses containing 20 mass% Na_2O . (B) The boundary is defined by the requirement that the glasses contain 25 mass% Na_2O . Solid lines represent $r_B = 1 \text{ g m}^{-2}$ and dashed lines $r_B = 2 \text{ g m}^{-2}$.

a single waste composition showing that the maximum loading of the waste (represented by the Na_2O content) together with the processability and acceptability criteria allow considerable variability of glass formulation. When the waste is occupying a region in the composition space instead of a single point, as in the examples above, the determination of the boundaries of the corresponding glass composition region is more challenging. One of the pitfalls in assessing such region in a multidimensional space for experimental studies is the “dimensionality curse” [17].

4.2. PCT limitations in assessing long-term alteration

According to Gin et al. [7], nuclear waste glass powder immersed in water in a closed container initially alters at a high constant rate, dubbed the initial rate. This stage is followed by a period of decreasing alteration rate (the rate-drop period). The final rate, called the residual rate, is nearly constant until all glass is altered, though for some glasses under some conditions the rate may temporarily accelerate before achieving residual rate.

For different glasses, the alteration process may progress through stages of different duration and extent. The solution compositions and pH change during the PCT-type tests (Gin et al. [7] used buffered solutions) and the extent of these changes differs

for different glass compositions. Finally, the alteration layers that form on the glass–solution interface may differ in structure and properties from glass to glass. These effects cannot be discerned by a single test, such as the seven-day PCT. Yet drastic limitations are inevitable for a study aimed at determining the effects of glass composition variation over an extensive composition region. Such study may help identify areas for future in-depth research aimed at exploring the effects of variables important for the long-term alteration.

Suppose that the long-term alteration of nuclear waste glass can be represented by a simple heuristic model

$$r = r_1 \tanh \frac{t}{t_0} + \dot{r}_r t \quad (2)$$

where \tanh is the hyperbolic tangent, r is the B normalized release (dropping the subscript B), t is the time, t_0 is the rate-drop time constant, r_1 is a constant that equal to t_0 times the initial rate minus the residual rate, see below, the dot above the symbol indicates the time derivative (the rate), and the subscript r stands for “residual.”

By Eq. (2), the alteration rate is $dr/dt = \dot{r} = (r_1/t_0)[\cosh(t/t_0)]^{-2} + \dot{r}_r$. Thus, the initial rate ($\dot{r}_0 = r_1/t_0 + \dot{r}_r$), the final rate (\dot{r}_r), and the rate-drop stage duration, which is proportional to t_0 , are independent parameters. This is in agreement with Gin et al. [7], who did not find any obvious relationship between the initial and residual rates.

Fig. 7 plots the alteration rate versus time through the rate-drop period for a variety of r_1 and t_0 values while leaving the residual rate at a constant value of $1.5 \times 10^{-4} \text{ g m}^{-2} \text{ d}^{-1}$. The seven-day PCT response (in terms of the normalized B release) is the same,

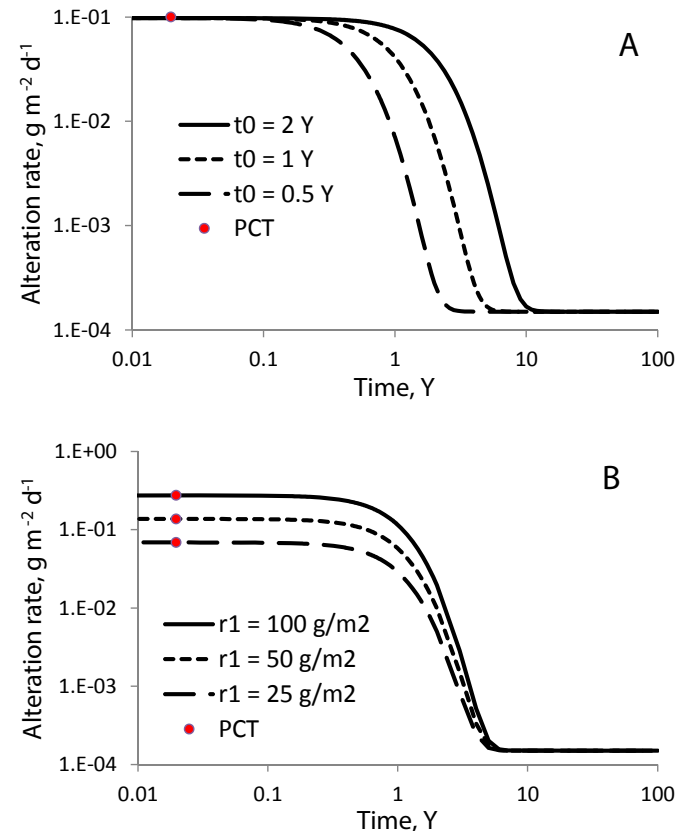


Fig. 7. Glass alteration rate versus time based on Eq. (2). (A) The curves are drawn for three values of the time constant (shown in the legend) and $r_{\text{PCT}} = 0.7 \text{ g m}^{-2}$. (B) The curves are drawn for three values of r_1 (shown in the legend) and $t_0 = 1 \text{ Y}$.

$r_{PCT} = 0.7 \text{ g m}^{-2}$, for each curve in Fig. 7A. Omitting the small term $\dot{r}_r t_{PCT}$, we get $r_1 = r_{PCT}/\tanh(t_{PCT}/t_0)$. On a scale of years (Y), $t_{PCT} = 0.02 \text{ Y}$. During this period, the alteration rate is virtually constant and indistinguishable from \dot{r}_0 . Accordingly, $\dot{r}_0 \approx r_{PCT}/t_{PCT}$, so the PCT response can be used (for this set of parameters) as a rough estimate for the initial rate of alteration. This assessment is in agreement with Frugier et al. [14] method of the initial alteration rate determination. They used a Soxhlet instrument exposing a polished coupon to $100 \text{ }^\circ\text{C}$ for 3–28 days. For R7T7 type glasses, the average was $\dot{r}_0 = 2.4 \text{ g m}^{-2} \text{ d}^{-1}$, which reasonably compares with the average of $1.7 \text{ g m}^{-2} \text{ d}^{-1}$ for our glasses. In Fig. 7B, the initial alteration rate is allowed to vary.

With a minimum of three parameters, as in Eq. (2), at least two more data points are needed to get the full \dot{r} vs. t (or r vs. t) relationship. As indicated in Fig. 7, the seven-day PCT, or a similar experiment, provides just one point on the \dot{r} vs. t curve that would not tell us much about the rate-drop period except imposing a limit on the total release during that period, but only when the process is sufficiently simple (no acceleration occurs, etc.). The only relationship that may exist between \dot{r}_0 and \dot{r}_r is that both are related to glass composition.

5. Conclusions

1) As has been documented on glasses containing varying fractions of SiO_2 , B_2O_3 , CaO , Al_2O_3 , and ZrO_2 with and without Li_2O , the response of initial alteration rate to an increasing fraction of Na_2O is simple and monotonous until the final loss of chemical durability at high Na_2O fraction (as high as 30 mass%). Consequently, a threshold at which glass structure would abruptly fall

apart or beyond which a continuous nondurable phase would be separated is unlikely to occur in multicomponent waste glasses.

2) The outcome of this research confirms and quantifies various phenomena; for example:

- The normalized release of Na becomes increasingly lower than the normalized release of B as the glass becomes more nondurable.
- Alumina exhibits a powerful positive impact on the initial rate of alteration of alkali-containing glasses.
- CaO assumes a special role with respect to the PCT response and melt viscosity, a feature advantageous in formulating acceptable glasses for nuclear waste vitrification.

Acknowledgments

We are grateful to the Division of Advanced Nuclear Engineering (DANE) (R31-3005) of Pohang University of Science and Technology (POSTECH) for providing all the required facilities and funds to perform this research. The authors gratefully acknowledge that this work was supported by the BK21 + program through the National Research Foundation of Korea funded by the Ministry of Education, Science and Technology. P. Hrma greatly appreciates the financial support of the U.S. Department of Energy's Hanford Tank Waste Treatment and Immobilization Plant Federal Project Office under the direction of A.A. Kruger.

Appendix. Glass compositions and PCT data

Table A1

Composition of Li-containing test glasses in mass fractions of oxides and normalized 7-day PCT B and Na releases in g m^{-2} .

ID	SiO_2	B_2O_3	Al_2O_3	ZrO_2	CaO	Na_2O	Li_2O	r_B	r_{Na}
CT-S50-N30	0.4268	0.1024	0.0427	0.0512	0.0341	0.3000	0.0427	62.65	44.70
CT-S50-N28	0.4390	0.1054	0.0439	0.0527	0.0351	0.2800	0.0439	50.66	33.36
CT-S50-N26	0.4512	0.1083	0.0451	0.0541	0.0361	0.2600	0.0451	48.93	31.99
CT-S50-N24	0.4634	0.1112	0.0463	0.0556	0.0371	0.2400	0.0463	22.08	15.84
CT-S50-N22	0.4756	0.1141	0.0476	0.0571	0.0380	0.2200	0.0476	10.01	7.22
CT-S50-N20	0.4878	0.1171	0.0488	0.0585	0.0390	0.2000	0.0488	6.14	5.72
CT-S50-N18	0.5000	0.1200	0.0500	0.0600	0.0400	0.1800	0.0500	4.07	4.35
CT-S50-N16	0.5122	0.1229	0.0512	0.0615	0.0410	0.1600	0.0512	4.36	5.89
CT-S50-N14	0.5244	0.1259	0.0524	0.0629	0.0420	0.1400	0.0524	4.27	4.52
CT-S40-N30	0.3415	0.1404	0.0585	0.0702	0.0468	0.3000	0.0427	53.79	39.25
CT-S40-N28	0.3512	0.1444	0.0602	0.0722	0.0481	0.2800	0.0439	31.47	22.16
CT-S40-N26	0.3610	0.1484	0.0618	0.0742	0.0495	0.2600	0.0451	21.66	13.22
CT-S40-N24	0.3707	0.1524	0.0635	0.0762	0.0508	0.2400	0.0463	16.62	12.55
CT-S40-N22	0.3805	0.1564	0.0652	0.0782	0.0521	0.2200	0.0476	9.18	9.01
CT-S40-N20	0.3902	0.1604	0.0668	0.0802	0.0535	0.2000	0.0488	7.43	7.8
CT-S40-N18	0.4000	0.1644	0.0685	0.0822	0.0548	0.1800	0.0500	5.75	5.57
CT-S40-N16	0.4098	0.1685	0.0702	0.0842	0.0562	0.1600	0.0512	4.30	5.03
CT-S40-N14	0.4195	0.1725	0.0719	0.0862	0.0575	0.1400	0.0524	4.62	4.43
CT-S35-N28	0.3073	0.1639	0.0683	0.0820	0.0546	0.2800	0.0439	23.44	17.81
CT-S35-N26	0.3159	0.1685	0.0702	0.0842	0.0562	0.2600	0.0451	26.09	10.68
CT-S35-N24	0.3244	0.1730	0.0721	0.0865	0.0577	0.2400	0.0463	25.12	19.10
CT-S35-N22	0.3329	0.1776	0.0740	0.0888	0.0592	0.2200	0.0476	8.78	8.74
CT-S35-N20	0.3415	0.1821	0.0759	0.0911	0.0607	0.2000	0.0488	6.54	6.32
CT-S35-N18	0.3500	0.1867	0.0778	0.0933	0.0622	0.1800	0.0500	5.91	5.68
CT-S35-N16	0.3585	0.1912	0.0797	0.0956	0.0637	0.1600	0.0512	4.61	5.39
CT-S35-N14	0.3671	0.1958	0.0816	0.0979	0.0653	0.1400	0.0524	4.80	4.61
CT-B16-N28	0.4120	0.1405	0.0412	0.0494	0.0330	0.2800	0.0439	48.52	33.24
CT-B16-N26	0.4235	0.1444	0.0423	0.0508	0.0339	0.2600	0.0451	56.71	43.78
CT-B16-N24	0.4349	0.1483	0.0435	0.0522	0.0348	0.2400	0.0463	33.12	22.45
CT-B16-N22	0.4463	0.1522	0.0446	0.0536	0.0357	0.2200	0.0476	29.24	20.11
CT-B16-N20	0.4578	0.1561	0.0458	0.0549	0.0366	0.2000	0.0488	14.27	11.6
CT-B16-N18	0.4692	0.1600	0.0469	0.0563	0.0375	0.1800	0.0500	8.81	8.31
CT-B16-N16	0.4807	0.1639	0.0481	0.0577	0.0385	0.1600	0.0512	10.74	9.33
CT-B16-N14	0.4921	0.1678	0.0492	0.0591	0.0394	0.1400	0.0524	7.95	5.29
CT-B16-N12	0.5036	0.1717	0.0504	0.0604	0.0403	0.1200	0.0537	7.92	6.72
CT-B08-N28	0.4660	0.0702	0.0466	0.0559	0.0373	0.2800	0.0439	36.1	24.07
CT-B08-N26	0.4790	0.0722	0.0479	0.0575	0.0383	0.2600	0.0451	32.34	5.94

(continued on next page)

Table A1 (continued)

ID	SiO ₂	B ₂ O ₃	Al ₂ O ₃	ZrO ₂	CaO	Na ₂ O	Li ₂ O	r _B	r _{Na}
CT-B08-N24	0.4919	0.0741	0.0492	0.0590	0.0394	0.2400	0.0463	3.32	3.81
CT-B08-N22	0.5049	0.0761	0.0505	0.0606	0.0404	0.2200	0.0476	3.21	3.73
CT-B08-N20	0.5178	0.0780	0.0518	0.0621	0.0414	0.2000	0.0488	2.88	4.28
CT-B08-N18	0.5308	0.0800	0.0531	0.0637	0.0425	0.1800	0.0500	3.47	6.98
CT-B08-N16	0.5437	0.0820	0.0544	0.0652	0.0435	0.1600	0.0512	1.87	3.36
CT-B08-N14	0.5567	0.0839	0.0557	0.0668	0.0445	0.1400	0.0524	2.12	3.77
CT-A08-N28	0.4207	0.1010	0.0702	0.0505	0.0337	0.2800	0.0439	61.13	35.87
CT-A08-N26	0.4324	0.1038	0.0722	0.0519	0.0346	0.2600	0.0451	25.90	5.57
CT-A08-N24	0.4441	0.1066	0.0741	0.0533	0.0355	0.2400	0.0463	3.51	5.14
CT-A08-N22	0.4558	0.1094	0.0761	0.0547	0.0365	0.2200	0.0476	3.44	4.33
CT-A08-N20	0.4675	0.1122	0.0780	0.0561	0.0374	0.2000	0.0488	4.30	5.30
CT-A08-N18	0.4792	0.1150	0.0800	0.0575	0.0383	0.1800	0.0500	3.30	4.02
CT-A08-N16	0.4909	0.1178	0.0820	0.0589	0.0393	0.1600	0.0512	4.20	5.05
CT-A11-N28	0.4024	0.0966	0.0966	0.0483	0.0322	0.2800	0.0439	4.40	7.61
CT-A11-N26	0.4136	0.0993	0.0993	0.0496	0.0331	0.2600	0.0451	2.25	3.30
CT-A11-N24	0.4248	0.1020	0.1020	0.0510	0.0340	0.2400	0.0463	2.56	3.79
CT-A11-N22	0.4360	0.1046	0.1046	0.0523	0.0349	0.2200	0.0476	2.36	3.34
CT-A11-N20	0.4472	0.1073	0.1073	0.0537	0.0358	0.2000	0.0488	1.90	2.68
CT-A11-N18	0.4583	0.1100	0.1100	0.0550	0.0367	0.1800	0.0500	2.84	4.05
CT-Z03-N28	0.4576	0.1098	0.0458	0.0263	0.0366	0.2800	0.0439	53.21	36.49
CT-Z03-N26	0.4703	0.1129	0.0470	0.0271	0.0376	0.2600	0.0451	21.39	20.10
CT-Z03-N24	0.4830	0.1159	0.0483	0.0278	0.0386	0.2400	0.0463	49.71	36.45
CT-Z03-N22	0.4957	0.1190	0.0496	0.0285	0.0397	0.2200	0.0476	28.83	4.30
CT-Z03-N20	0.5084	0.1220	0.0508	0.0293	0.0407	0.2000	0.0488	2.12	3.26
CT-Z03-N18	0.5211	0.1251	0.0521	0.0300	0.0417	0.1800	0.0500	2.28	2.94
CT-Z03-N16	0.5338	0.1281	0.0534	0.0307	0.0427	0.1600	0.0512	2.50	3.04
CT-Z03-N14	0.5465	0.1312	0.0547	0.0315	0.0437	0.1400	0.0524	2.96	3.47
CT-Z09-N28	0.4205	0.1009	0.0420	0.0790	0.0336	0.2800	0.0439	40.61	27.68
CT-Z09-N26	0.4322	0.1037	0.0432	0.0812	0.0346	0.2600	0.0451	36.49	14.41
CT-Z09-N24	0.4438	0.1065	0.0444	0.0834	0.0355	0.2400	0.0463	16.42	13.52
CT-Z09-N22	0.4555	0.1093	0.0456	0.0856	0.0364	0.2200	0.0476	11.96	15.46
CT-Z09-N20	0.4672	0.1121	0.0467	0.0878	0.0374	0.2000	0.0488	6.62	6.45
CT-Z09-N18	0.4789	0.1149	0.0479	0.0900	0.0383	0.1800	0.0500	6.78	5.72
CT-Z09-N16	0.4906	0.1177	0.0491	0.0922	0.0392	0.1600	0.0512	4.19	5.00
CT-Z09-N14	0.5022	0.1205	0.0502	0.0944	0.0402	0.1400	0.0524	3.63	3.96
CT-Z09-N12	0.5139	0.1233	0.0514	0.0966	0.0411	0.1200	0.0537	3.92	3.64
CT-C00-N28	0.4631	0.1111	0.0463	0.0556	0.0000	0.2800	0.0439	52.81	35.96
CT-C00-N26	0.4759	0.1142	0.0476	0.0571	0.0000	0.2600	0.0451	64.01	44.38
CT-C00-N24	0.4888	0.1173	0.0489	0.0587	0.0000	0.2400	0.0463	50.19	37.77
CT-C00-N22	0.5017	0.1204	0.0502	0.0602	0.0000	0.2200	0.0476	41.01	30.70
CT-C00-N20	0.5145	0.1235	0.0515	0.0617	0.0000	0.2000	0.0488	28.87	21.08
CT-C00-N18	0.5274	0.1266	0.0527	0.0633	0.0000	0.1800	0.0500	25.02	16.37
CT-C00-N16	0.5403	0.1297	0.0540	0.0648	0.0000	0.1600	0.0512	27.77	19.22
CT-C00-N14	0.5531	0.1327	0.0553	0.0664	0.0000	0.1400	0.0524	13.97	8.87
CT-C00-N12	0.5660	0.1358	0.0566	0.0679	0.0000	0.1200	0.0537	13.09	8.65
CT-C00-N10	0.5789	0.1389	0.0579	0.0695	0.0000	0.1000	0.0549	5.55	2.53
CT-C00-N08	0.5917	0.1420	0.0592	0.0710	0.0000	0.0800	0.0561	4.81	1.29
CT-C08-N28	0.4150	0.0996	0.0415	0.0498	0.0702	0.2800	0.0439	55.74	37.50
CT-C08-N26	0.4265	0.1024	0.0426	0.0512	0.0722	0.2600	0.0451	18.03	16.10
CT-C08-N24	0.4380	0.1051	0.0438	0.0526	0.0741	0.2400	0.0463	5.71	6.16
CT-C08-N22	0.4495	0.1079	0.0450	0.0539	0.0761	0.2200	0.0476	3.50	4.04
CT-C08-N20	0.4611	0.1107	0.0461	0.0553	0.0780	0.2000	0.0488	4.52	3.51
CT-C08-N18	0.4726	0.1134	0.0473	0.0567	0.0800	0.1800	0.0500	1.63	2.38
CT-C08-N16	0.4841	0.1162	0.0484	0.0581	0.0820	0.1600	0.0512	3.13	3.48

Table A2

Composition of Li-free test glasses in mass fractions of oxides and the normalized 7-day PCT B and Na releases in g m⁻².

ID	SiO ₂	B ₂ O ₃	Al ₂ O ₃	ZrO ₂	CaO	Na ₂ O	r _B	r _{Na}
CT-S50-N23	0.5000	0.1200	0.0500	0.0600	0.0400	0.2300	3.34	3.62
CT-S50-N21	0.5130	0.1231	0.0513	0.0616	0.0410	0.2100	3.13	2.78
CT-S50-N19	0.5260	0.1262	0.0526	0.0631	0.0421	0.1900	2.46	1.98
CT-S50-N17	0.5390	0.1294	0.0539	0.0647	0.0431	0.1700	0.91	0.84
CT-S50-N15	0.5519	0.1325	0.0552	0.0662	0.0442	0.1500	0.47	0.52
CT-S40-N23	0.4000	0.1644	0.0685	0.0822	0.0548	0.2300	4.67	3.60
CT-S40-N21	0.4104	0.1687	0.0703	0.0844	0.0562	0.2100	5.77	3.98
CT-S40-N19	0.4208	0.1730	0.0721	0.0865	0.0577	0.1900	3.07	2.37
CT-S40-N17	0.4312	0.1773	0.0739	0.0886	0.0591	0.1700	1.78	1.31
CT-S40-N15	0.4416	0.1815	0.0756	0.0908	0.0605	0.1500	0.11	0.078
CT-S35-N23	0.3500	0.1867	0.0778	0.0933	0.0622	0.2300	5.05	4.05
CT-S35-N21	0.3591	0.1915	0.0798	0.0958	0.0638	0.2100	4.90	3.77
CT-S35-N19	0.3682	0.1964	0.0818	0.0982	0.0655	0.1900	4.28	3.30
CT-S35-N17	0.3773	0.2012	0.0838	0.1006	0.0671	0.1700	2.79	2.15
CT-S35-N15	0.3864	0.2061	0.0859	0.1030	0.0687	0.1500	1.79	1.16

Table A2 (continued)

ID	SiO ₂	B ₂ O ₃	Al ₂ O ₃	ZrO ₂	CaO	Na ₂ O	r _B	r _{Na}
CT-B16-N23	0.4692	0.1600	0.0469	0.0563	0.0375	0.2300	8.24	5.87
CT-B16-N21	0.4814	0.1642	0.0481	0.0578	0.0385	0.2100	6.40	5.66
CT-B16-N19	0.4936	0.1683	0.0494	0.0592	0.0395	0.1900	3.70	3.31
CT-B16-N17	0.5058	0.1725	0.0506	0.0607	0.0405	0.1700	2.92	2.18
CT-B16-N15	0.5180	0.1766	0.0518	0.0622	0.0414	0.1500	2.31	1.59
CT-B08-N23	0.5308	0.0800	0.0531	0.0637	0.0425	0.2300	1.95	1.74
CT-B08-N21	0.5446	0.0821	0.0545	0.0653	0.0436	0.2100	1.40	2.03
CT-B08-N19	0.5583	0.0842	0.0558	0.0670	0.0447	0.1900	1.23	1.28
CT-B08-N17	0.5721	0.0862	0.0572	0.0687	0.0458	0.1700	0.33	0.46
CT-B08-N15	0.5859	0.0883	0.0586	0.0703	0.0469	0.1500	0.19	0.37
CT-A08-N23	0.4792	0.1150	0.0800	0.0575	0.0383	0.2300	1.83	3.77
CT-A08-N21	0.4916	0.1180	0.0821	0.0590	0.0393	0.2100	1.19	1.11
CT-A08-N19	0.5041	0.1210	0.0842	0.0605	0.0403	0.1900	0.41	0.56
CT-A08-N17	0.5165	0.1240	0.0862	0.0620	0.0413	0.1700	0.30	0.40
CT-A08-N15	0.5290	0.1269	0.0883	0.0635	0.0423	0.1500	0.32	0.32
CT-A11-N23	0.4583	0.1100	0.1100	0.0550	0.0367	0.2300	0.80	1.22
CT-A11-N21	0.4702	0.1129	0.1129	0.0564	0.0376	0.2100	0.45	0.59
CT-A11-N19	0.4821	0.1157	0.1157	0.0579	0.0386	0.1900	0.31	0.46
CT-A11-N17	0.4940	0.1186	0.1186	0.0593	0.0395	0.1700	0.22	0.35
CT-A11-N15	0.5060	0.1214	0.1214	0.0607	0.0405	0.1500	0.21	0.30
CT-Z03-N23	0.5211	0.1251	0.0521	0.0300	0.0417	0.2300	2.62	2.64
CT-Z03-N21	0.5347	0.1283	0.0535	0.0308	0.0428	0.2100	2.34	2.20
CT-Z03-N19	0.5482	0.1316	0.0548	0.0316	0.0439	0.1900	1.69	1.43
CT-Z03-N17	0.5617	0.1348	0.0562	0.0323	0.0449	0.1700	1.64	1.29
CT-Z03-N15	0.5753	0.1381	0.0575	0.0331	0.0460	0.1500	1.69	0.91
CT-Z09-N23	0.4789	0.1149	0.0479	0.0900	0.0383	0.2300	3.39	3.15
CT-Z09-N21	0.4913	0.1179	0.0491	0.0923	0.0393	0.2100	2.76	2.36
CT-Z09-N19	0.5037	0.1209	0.0504	0.0947	0.0403	0.1900	1.27	0.37
CT-Z09-N17	0.5162	0.1239	0.0516	0.0970	0.0413	0.1700	0.25	0.20
CT-Z09-N15	0.5286	0.1269	0.0529	0.0994	0.0423	0.1500	0.40	0.40
CT-C00-N23	0.5274	0.1266	0.0527	0.0633	0.0000	0.2300	12.37	6.85
CT-C00-N21	0.5411	0.1299	0.0541	0.0649	0.0000	0.2100	3.04	1.90
CT-C00-N19	0.5548	0.1332	0.0555	0.0666	0.0000	0.1900	0.49	0.52
CT-C00-N17	0.5685	0.1364	0.0568	0.0682	0.0000	0.1700	0.47	0.40
CT-C00-N15	0.5822	0.1397	0.0582	0.0699	0.0000	0.1500	0.15	0.36
CT-C08-N23	0.4726	0.1134	0.0473	0.0567	0.0800	0.2300	1.77	2.34
CT-C08-N21	0.4849	0.1163	0.0485	0.0582	0.0821	0.2100	1.40	2.10
CT-C08-N19	0.4972	0.1193	0.0498	0.0596	0.0842	0.1900	1.27	1.42
CT-C08-N17	0.5094	0.1222	0.0510	0.0611	0.0862	0.1700	0.29	0.51
CT-C08-N15	0.5217	0.1252	0.0522	0.0626	0.0883	0.1500	0.62	0.68

References

- [1] S. Gin, P. Jollivet, M. Fournier, C. Berthon, Z. Wang, A. Mitroshkov, Z. Zhu, J.V. Ryan, The fate of silicon during glass corrosion under alkaline conditions: a mechanistic and kinetic study with the international simple glass, *Geochim. Cosmochim. Acta* 151 (2015) 68–85.
- [2] S. Gin, P. Jollivet, M. Fournier, F. Angeli, P. Frugier, T. Charpentier, Origin and consequences of silicate glass passivation by surface layers, *Nat. Commun.* 6 (2015) 6360. <http://dx.doi.org/10.1038/ncomms7360>.
- [3] J.D. Vienna, J.V. Ryan, S. Gin, Y. Inagaki, Current understanding and remaining challenges in modeling long-term degradation of borosilicate nuclear waste glasses, *Int. J. Appl. Glass Sci.* 4 (2013) 283–294.
- [4] T. Maeda, K. Hotta, H. Usui, T. Banba, Characteristics of alteration layers formed on simulated HLW glass under silica-saturated solutions, *J. Aust. Ceram. Soc.* 48 (2012) 90–95.
- [5] A.C. Wright, Crystalline-like ordering in melt-quenched network glasses? *J. Non-Cryst. Solids* 401 (2014) 4–26.
- [6] R.J. Hand, A.B. Seddon, An hypothesis on the nature of griffith's cracks in alkali silicate and silica glasses, *Phys. Chem. Glas.* 38 (1997) 11–14.
- [7] S. Gin, X. Beaudoux, F. Angeli, C. Jegou, N. Godon, Effect of composition on the short-term and long-term dissolution rates of ten borosilicate glasses of increasing complexity from 3 to 30 oxides, *J. Non-Cryst. Solids* 358 (2012) 2559–2570.
- [8] M. Fournier, S. Gin, P. Frugier, Resumption of nuclear glass alteration: State of the art, *J. Nucl. Mater.* 448 (2014) 348–363.
- [9] E. Vernaz, S. Gin, C. Jegou, I. Ribet, Present understanding of R7T7 glass alteration kinetics and their impact on long-term behavior modeling, *J. Nucl. Mater.* 298 (2001) 27–36.
- [10] J.D. Vienna, D.S. Kim, D.C. Skorski, J. Matyas, Glass Property Models and Constraints for Estimating the Glass to Be Produced at Hanford by Implementing Current Advanced Glass Formulation Efforts, PNNL-22631, Rev. 1, ORP-58289, Pacific Northwest National Laboratory, Richland, WA, July, 2013.
- [11] S. Gin, A. Abdelouas, L.J. Criscenti, W.L. Ebert, K. Ferrand, T. Geisler, M.T. Harrison, Y. Inagaki, S. Mitsui, K.T. Mueller, J.C. Marra, C.G. Pantano, E.M. Pierce, J.V. Ryan, J.M. Schofield, C.I. Steefel, J.D. Vienna, An international initiative on long-term behavior of high-level nuclear waste glass, *Mater. Today* 16 (2013) 243–248.
- [12] C1285 e 14 ASTM, Standard Test Methods for Determining Chemical Durability of Nuclear, Hazardous, and Mixed Waste Glasses and Multiphase Glass Ceramics: the Product Consistency Test (PCT), ASTM International, West Conshohocken, PA, 2008.
- [13] A. Ledieu, F. Devreux, P. Barboux, L. Sicard, O. Spalla, Leaching of borosilicate glasses, I. Experiments, *J. Non-Cryst. Solids* 343 (2004) 3–12.
- [14] P. Frugier, C. Martin, I. Ribet, T. Advocat, S. Gin, The effect of composition on the leaching of three nuclear waste glasses: R7T7, AVM and VRZ, *J. Non-Cryst. Solids* 346 (2005) 194–207.
- [15] P. Hrma, A.A. Kruger, High-temperature viscosity of many-component glass melts, *J. Non-Cryst. Solids* 437 (2016) 17–25.
- [16] R.U. Farooqi, P. Hrma, Nonlinear relationship between the Product Consistency Test (PCT) response and the Al/B ratio in a soda-lime aluminoborosilicate glass, *J. Nucl. Mater.* 474 (2016) 28–34.
- [17] R.E. Bellman, *Dynamic Programming*, Courier Dover, 2003.